Electronic Supplementary Material (ESI) for Journal of Materials Chemistry A.
This journal is © The Royal Society of Chemistry 2020

Supporting Information

Seawater-responsive SiO_2 nanoparticles for *in situ* generation of zwitterionic PDMS antifouling coatings with underwater superoleophobicity

Jinyan Tan,[a] Jiakang Xu,[b] Donghui Wang,[a] Jinlong Yang,[*b] and Shuxue Zhou[*a]

[a]*Department of Materials Science, State Key Laboratory of Molecular Engineering of Polymers, Advanced Coatings Research Center of Ministry of Education of China, Fudan University, Shanghai 200433, China.*

[b]*International Research Center for Marine Biosciences, Ministry of Science and Technology, Shanghai Ocean University, Shanghai 201306, China.*

* Corresponding Authors

Jinlong Yang, E-mail: jlyang@shou.edu.cn

Shuxue Zhou, E-mail: zhoushuxue@fudan.edu.cn

Experimental Section

Materials:

(3-Aminopropyl)triethoxysilane (APS, 99%), methyl acrylate (MA, 99%, MEHQ stabilizer ≤ 100 ppm) were provided by Aladdin (China). Xylene (99%), anhydrous methanol (99.9%) and acetic acid (99.8%) were purchased from Sinopharm (China). Sylgard™ 184 (PDMS, base and curing agent) was the product of Dow Chemical Corporation (USA). Karstedt catalyst (20,000 ppm) was purchased from Shanghai Guiyou New Materials Technology Ltd. (China), and fumed silica (SiO_2-NPs, Aerosil 380) from Evonik (Germany). Deuterochloroform ($CDCl_3$, 99.8 atom% D, 0.03 volume% tetramethylsilane as internal standard) was purchased from Sigma-Aldrich (America). Fluorescein isothiocyanate-labelled bovine serum albumin (FITC-BSA) and crystal violet (0.1 wt.% aqueous solution) were provided by Solarbio Life Sciences Ltd. (China). Artificial seawater (ASW) was prepared according to ASTM D1141-98. Probe liquids for underwater oleophobicity: hexadecane (HD), cyclohexane, heptane, octane, decane, toluene, petroleum ether, liquid paraffin, dichloroethane, chloroform, kerosene, olive oil, castor oil, linseed oil, PMX-200, hexafluorobutyl methacrylate, fluorinert (FC-40, 3M), industrial grade pump oil and crude oil were all commercial products. Deionized water (DI) was used throughout all experiments.

Synthesis of MAPS and BMAPS:

MAPS and BMAPS were synthesized from APS and MA by *aza*-Michael addition, as illustrated in Figure 1b. In a typical procedure, APS (75.02 g, 0.34 mol) and MA (34.13 g, 0.40 mol) were added to a round-bottom flask equipped with a magnetic stirring bar. The mixture was stirred under N_2 purge at ambient temperature for 1 h. Then the solution was heated to 40 °C and kept for 72 h. The transparent liquid product, involving secondary amino groups, was the mono-adduct of APS, (*N*-methoxyacylethyl)-3-aminopropyltriethoxysilane (identified as MAPS). **^{1}H NMR** (400 MHz, $CDCl_3$, δ): 3.71 (s, 6H, O-C*H*$_2$-CH$_3$), 3.56 [s, 3H,

(C=O)-O-CH_3], 2.79-2.32 [m, 6H, $CH_2CH_2NHCH_2CH_2(C=O)$], 1.50 (s, br, 3H, $CH_2CH_2CH_2NHCH_2$), 1.11 (s, 9H, CH_3CH_2), 0.53 (s, 2H, Si-CH_2). Italic indicates the atom yielding the peak. **FT-IR** (KBr, cm^{-1}): 3330 (ν_s(N-H)), 2885-2970 (ν_s(C-H)), 1740 (ν_s(C=O)), 1550 (ν_b(N-H)). The di-adduct of APS was synthesized in similar manner as to afford bis(*N*-methoxyacylethyl)-3-aminopropyltriethoxysilane (identified as BMAPS) with tertiary amino groups. With the difference being that APS (55.34 g, 0.25 mol) and MA (53.81g, 0.63 mol) were fed and reacted for 7 d. Then the excess MA was evacuated by vacuum rotary evaporation (RV10, IKA, Germany) to yield transparent liquid product. **^{1}H NMR** (400 MHz, $CDCl_3$, δ): 3.76 (s, 6H, O-CH_2-CH_3), 3.59 [s, 6H, (C=O)-O-CH_3], 2.70-2.37 {d, 10H, $CH_2CH_2N[CH_2CH_2(C=O)]_2$}, 1.47 (s, 2H, $CH_2CH_2CH_2NHCH_2$), 1.15 (s, 9H, CH_3CH_2), 0.52 (s, 2H, Si-CH_2). **FT-IR** (KBr, cm^{-1}): 2885-2970 (ν_s(C-H)), 1740 (ν_s(C=O)).

Preparation of M-SiO_2 and BM-SiO_2:

SiO_2-NPs were dried under vacuum at 40 °C for 48 h before use. SiO_2-NP dispersion (4.5 wt.% in xylene, 145.00 g), MAPS or BMAPS (3.30 g) were added to a round-bottom flask. The reaction was conducted at 50 °C for 24 h. Then the slurry was centrifuged and washed with xylene for six times to get wet M-SiO_2 and BM-SiO_2 (corresponding to the modifier MAPS and BMAPS). The wet modified SiO_2 were dried under vacuum at 40 °C for 48 h or redispersed in xylene.

Fabrication of PDMS-based coatings:

M-SiO_2 (or BM-SiO_2) dispersion and PDMS base were blended by magnetic stirring (4 h, r.t.) and ultrasonication (53 kHz, 350 W, 30 min, r.t.) successively. Later, curing agent (10 wt.% of PDMS base) and Karstedt catalyst (3.5 wt.% of PDMS base) were charged into the mixture and stirred for another 30 min, followed by ultrasonication for 10 min. The mixture was sprayed on glass slides with a spray gun (Minijet 4400 B, SATA, Germany) at a spray distance of approx. 20 cm and a compressed air of approx. 0.6 MPa, then cured at 80 °C for 2 h. The coating samples were defined as PDMS/(B)M-SiO_2-*n*, where *n* represented the weight

percentage of nanofiller in dry coating (except curing agent and catalyst). PDMS/SiO_2-*n* coatings were fabricated in the same manner as PDMS/(B)M-SiO_2-*n* but bare SiO_2-NPs as nanofillers and without additional Karstedt catalyst.

Characterization:

The ^1H nuclear magnetic resonance (^1H NMR) spectra were recorded on an Avance III HD NMR spectrometer (400 MHz, Bruker, Germany). Fourier-transform infrared (FT-IR) spectra were obtained on a Nicolet 6700 spectrometer (Thermofisher, America) equipped with diamond attenuated total reflectance (ATR, Pike, America) and transmission sampling accessories. Thermogravimetric analyses (TGA) were carried out at a heating rate of 20 °C min^{-1}, under air atmosphere (O_2/N_2=1/4, flux: 40 mL min^{-1}), with a TGA Q500 instrument (TA, America). Morphology was observed by a field-emission scanning electron microscope (FE-SEM, Ultra 55, Carl Zeiss, Germany) equipped with an energy dispersive X-ray spectroscopy detector (EDX, X-Max 50, Oxford, England), at an accelerated voltage of 3 kV in secondary electron (SE2) mode. All the samples were coated with gold by a sputtering coater (Q150R, Quorum, England) prior to observation. Water contact angel (WCA), underwater oil contact angel (UWOCA) and underwater oil sliding angel (UWOSA) were measured with a contact angel goniometer (OCA25, DataPhysics, Germany). All measurements were carried out by injecting a 3 μL probe droplet with a screw-top syringe, and average values were obtained from five different regions of the same sample. Durability under harsh physical and chemical environment was conducted using the samples that had already achieved underwater superoleophobicity. The samples were exposed to acid (H_2SO_4 aqueous solution; pH = 1), alkali (NaOH aqueous solutions, pH = 10, 12) and high temperature (80 °C, 150 °C) for 10 d. Digital images and UWOCAs were acquired after exposure. Mechanical abrasion tests were carried out under ASW immersion, with the samples (38 × 26 mm^2) fixed in a ASW-filled tank (d = 190 mm). The coatings were facing upward and contact with a 1000-meshes sandpaper that bearing 500 g load. The sandpaper

was rubbed over the entire coatings along the longitudinal direction at a speed of approximately 4 cm s^{-1} (Movie S1†). After rubbing for 10 times, the UWOCA was checked, then immersed in ASW for 3 d, and later checked UWOCA and surface morphology. UV-vis transmittance spectra were recorded with resolution of 2 nm on an UV/Vis/NIR spectrophotometer (U-4100, Hitachi, Japan) equipped with an integrating sphere.

Laboratory AF assessments:

i) Protein adhesion assays: The anti-protein property was examined using FITC-BSA as a model protein foulant. Coating coupons (38 × 26 mm^2) were mounted into cell-culture dishes. FITC-BSA solution (4 mL, 20 μg mL^{-1} in phosphate-buffered saline (PBS), pH 7.4) was injected into each dish and incubated at 25 °C for 7 h in dark. Then, the solution was discarded and the panels were rinsed with fresh PBS buffer for five times to remove the free FITC-BSA. Confocal laser scanning microscopy (CLSM) images were recorded on a C2+ confocal microscope (Nikon, Japan), equipped with 488 nm laser excitation.

ii) Bacterial adhesion assays: Bacterial adhesion was carried out according to our previous report,[1] using *Pseudoalteromonas marina* as a model bacterial foulant. Three parallel coating coupons (38 × 26 mm^2) were put into sterilized Petri dishes. *P. marina* suspension (10^8 cells mL^{-1}) was added into each Petri dish and incubated at 18 °C for 48 h. Then, the panels were rinsed with 50 mL autoclaved filtered seawater (AFSW) to remove the free bacteria. The adhered bacteria on the panels were collected via ultrasonication, fixed by 5% formalin solution and stained by 0.1% acridine orange. The numbers of adhered bacteria were acquired by a fluorescent microscope, and average bacterial density values were obtained from ten different regions of each parallel coupon. Samples with and without prehydrolysis under AFSW for 2 d were both measured.

iii) Biofilm formation assays: Biofilm formation was carried out using crystal violet assay, with *P. marina* as a model foulant. Three parallel coating coupons (15 × 15 mm^2) were put into sterilized 12 well cell culture plate (Coster, Corning). *P. marina* suspension (10^8 cells

mL^{-1}) was added into each plate and incubated at 18 °C for 48 h. Then, the panels were rinsed with 50 mL AFSW to remove the free biofim. The adhered biofilm on the panels were fixed by methanol, stained by 0.1 wt.% crystal violet aqueous solution, and then rinsed with AFSW to remove free crystal violet. Later, the adhered crystal violet was extracted by 33 wt.% acetic acid aqueous solution, and quantified the biofilm formation by measuring the optical density (OD) values at 589 nm. Samples with and without prehydrolysis under AFSW for 2 d were both measured.

iv) Mussel settlement assays: Mussel settlement was carried out according to our previous report.[2] *Mytilus coruscus* plantigrades (Institute of Marine Science and Technology, Zhoushan, China) was cultured with a 2 L aerated beaker with 10 plantigrades/mL in AFSW under 18 °C. The culture medium was fed with *Isochrysis galbana* (10-20 × 10^4 cells mL^{-1} d^{-1}) and the AFSW was replaced every 24 h. The model plantigrade foulant *M. coruscus* (shell length: 0.71 ± 0.05 mm, shell height: 0.43 ± 0.06 mm) was acquired after cultured for more than one week. Nine parallel coating coupons (38 × 26 mm^2) were put into sterilized Petri dishes. *M. coruscus* plantigrades (10 mussels with 20 mL AFSW) were placed in each Petri dish and incubated for 48 h. Finally, the mussel settled on the panels by byssal threads was counted. Samples with and without prehydrolysis under AFSW for 2 d were both measured.

Marine field AF trials:

The marine field tests were conducted at East China Sea, Pacific Ocean (Hangzhou Bay, coordinates 122°46′ E, 30°43′ N) from September 26, 2019 to October 24, 2019. The coated glass slide panels with an approx. area of 38 × 26 mm^2 were immobilized within the custom-made molds and submerged at approx. 1 m in depth. After a certain period of time, the panels were taken out, carefully rinsed with seawater to remove unattached silt and biofouling, inspected with naked eyes and photographed, then immediately placed back into seawater. After terminating the submersion, the adhesion density of bacteria and diatoms were measured with three parallel replicates for each group. The biofilms on the panels were

collected via ultrasonication, fixed by 5% formalin solution and stained by 0.1% acridine orange. The numbers of adhered bacteria and diatoms were acquired by a fluorescent microscope, and average density values were obtained from ten different regions of the same panel. Mussel settlement of the coatings with biofilms formed under field exposure was measured similar as laboratory assessment. Finally, the morphology after field exposure for 14 d was additionally observed by KH-7700 optical microscope (OM, Hirox, America), DP26 OM (Olympus, Japan), and FE-SEM.

Figure S1

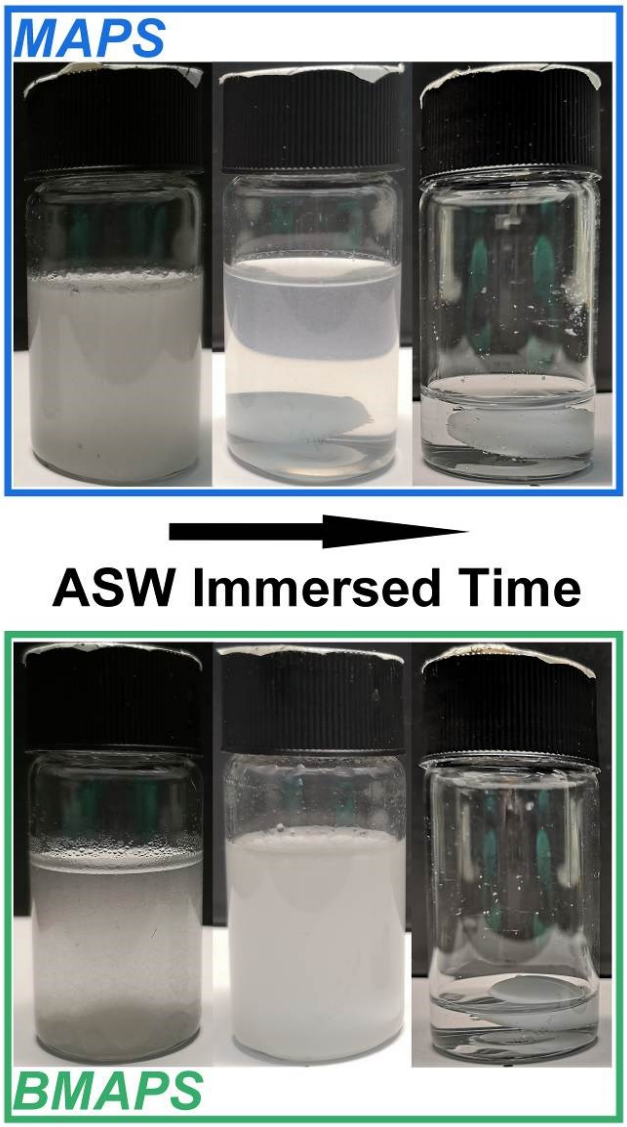

Fig. S1 Digital images recording the dynamic hydrolysis process of MAPS and BMAPS under ASW.

Figure S2

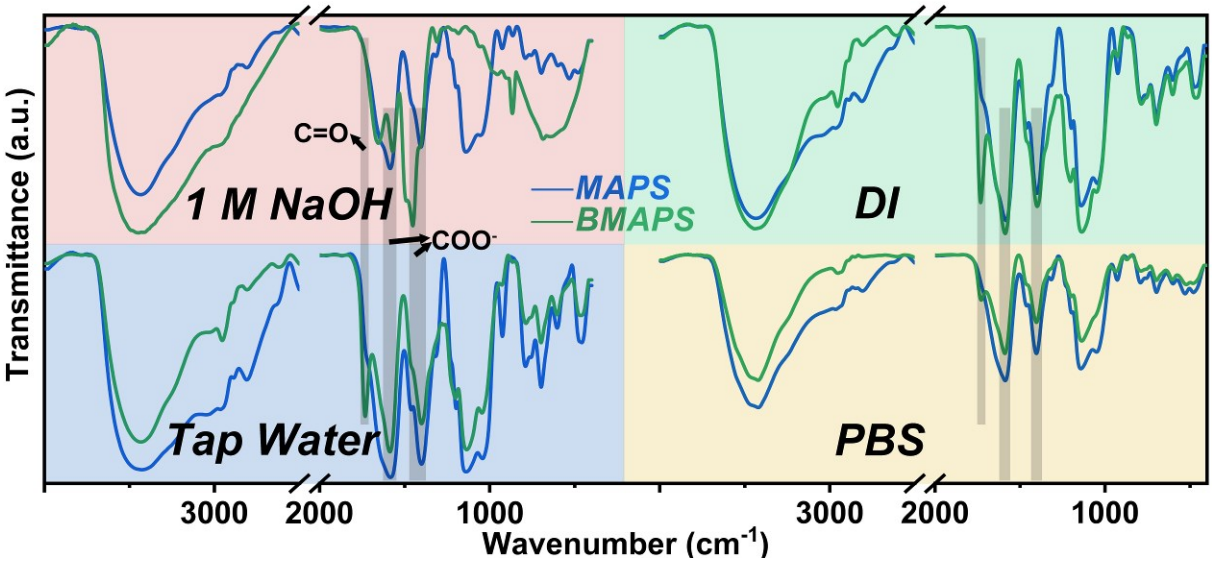

Fig. S2 FT-IR spectra (KBr, r.t.) recording the hydrolysis capability of MAPS and BMAPS under various media: 1 M NaOH aqueous solution, DI, tap water and PBS.

Figure S3

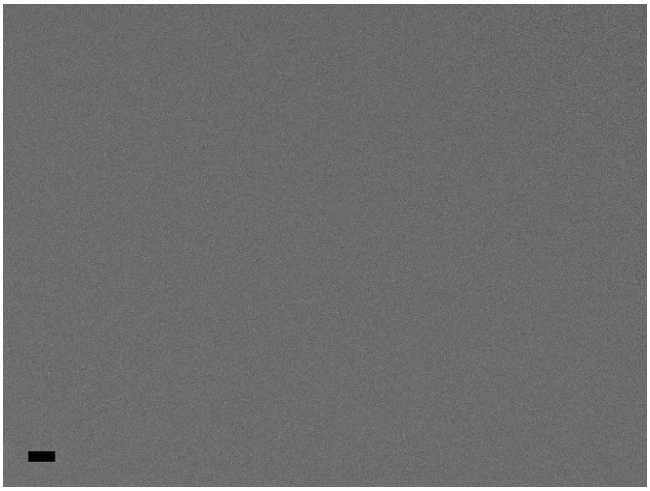

Fig. S3 FE-SEM image of PDMS coating. Scale bar: 10 μm.

Figure S4

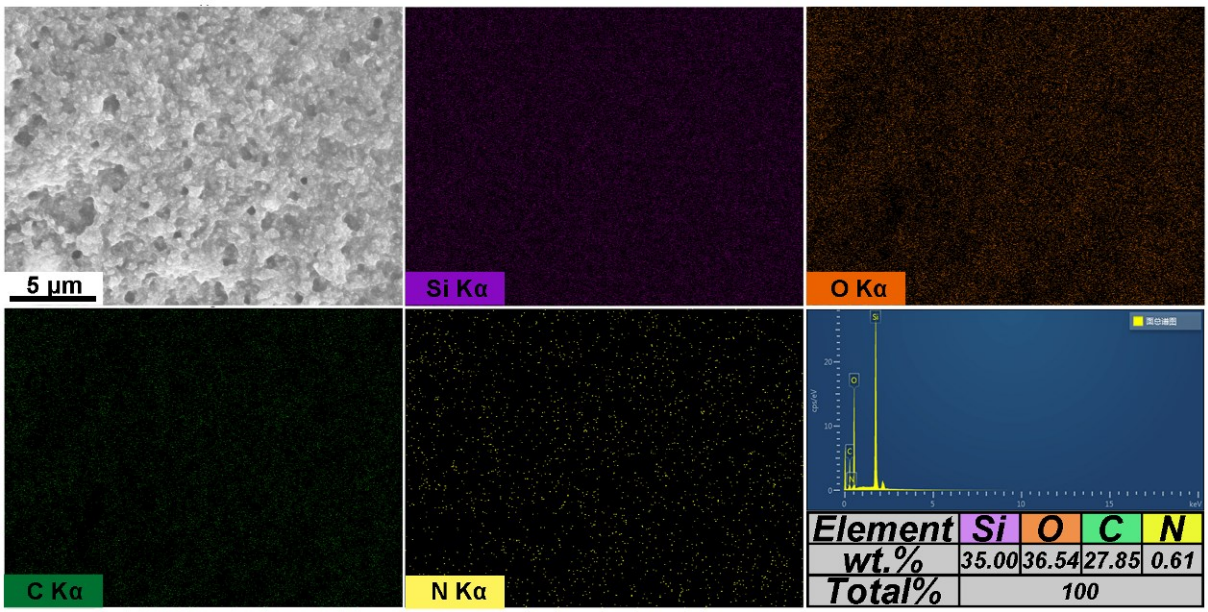

Fig. S4 EDX images of PDMS/BM-SiO_2-*30* with corresponding elemental mapping and the contents of Si, O, C, N. Scale bar is applicable to all images.

Figure S5

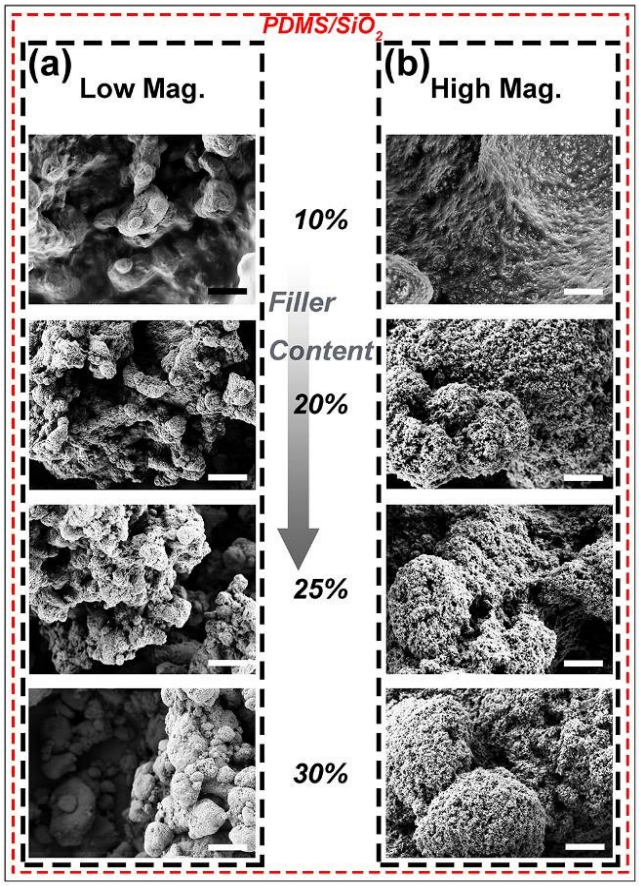

Fig. S5 FE-SEM images with a) low (scale bar: 20 μm) and b) high (scale bar: 2 μm) magnifications of PDMS/SiO_2-*n*.

Figure S6

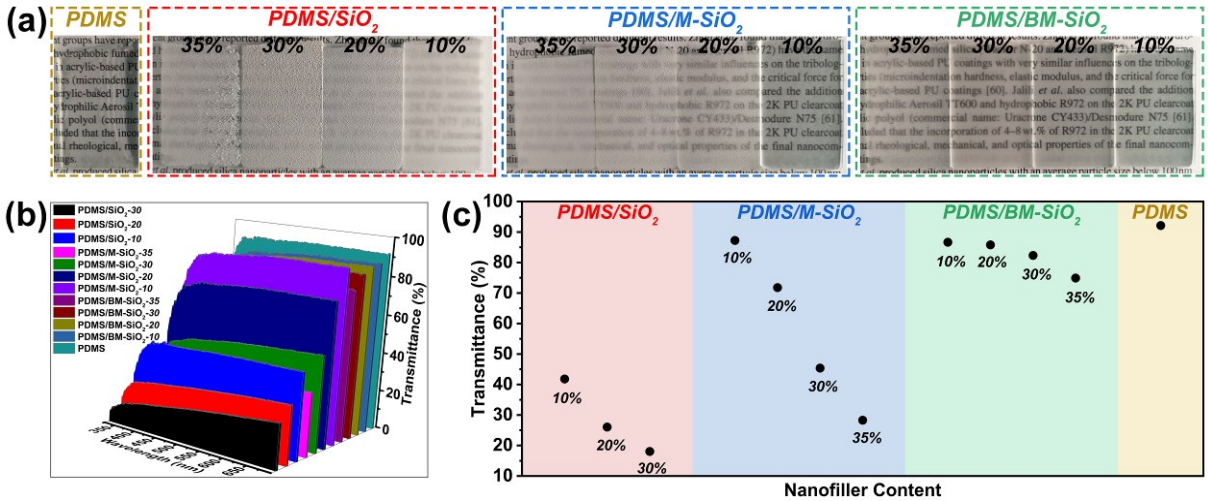

Fig. S6 Optical transparency. a) Digital images, b) UV-vis transmittance spectra, and c) typical transmittances at 550 nm of PDMS, PDMS/SiO_2 -*n*, PDMS/M-SiO_2-*n*, and PDMS/BM-SiO_2-*n*.

Figure S7

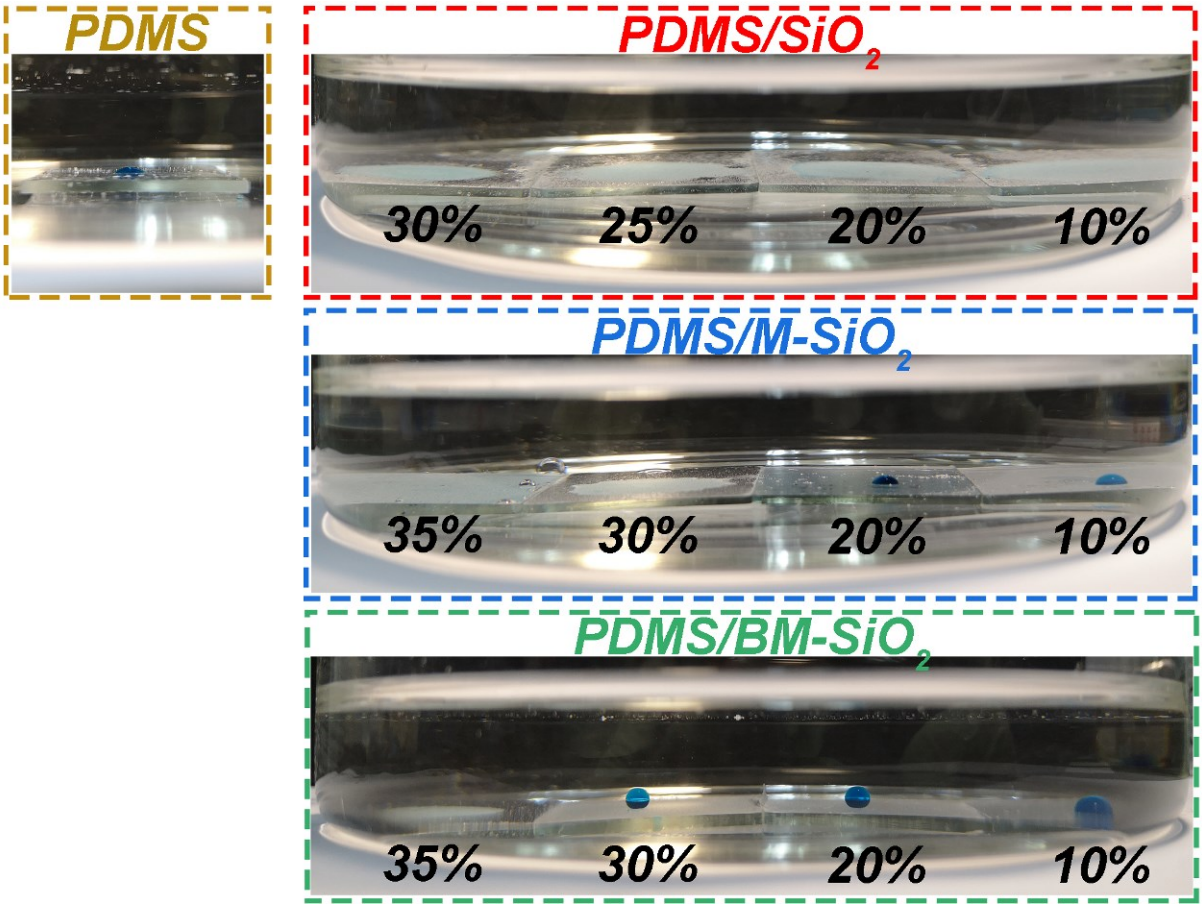

Fig. S7 Digital images of chloroform droplets (dyed blue) on the underwater surfaces of PDMS, PDMS/SiO_2-*n*, PDMS/M-SiO_2-*n*, and PDMS/BM-SiO_2-*n*.

Figure S8

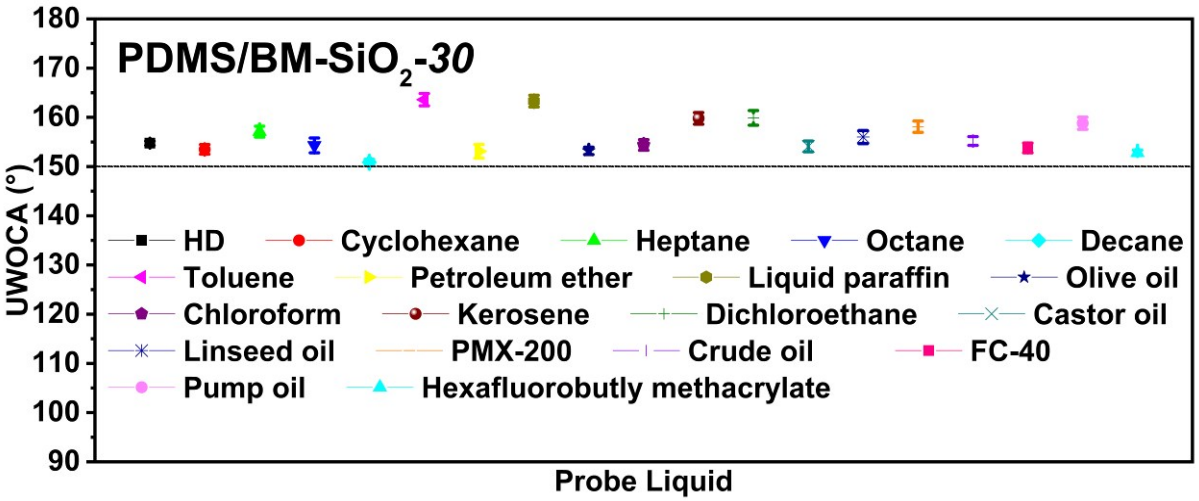

Fig. S8 UWOCAs towards various oily liquids on the surface of PDMS/BM-SiO_2-*30* after immersed in ASW for 3 d (mean ± SD, $n = 5$).

Figure S9

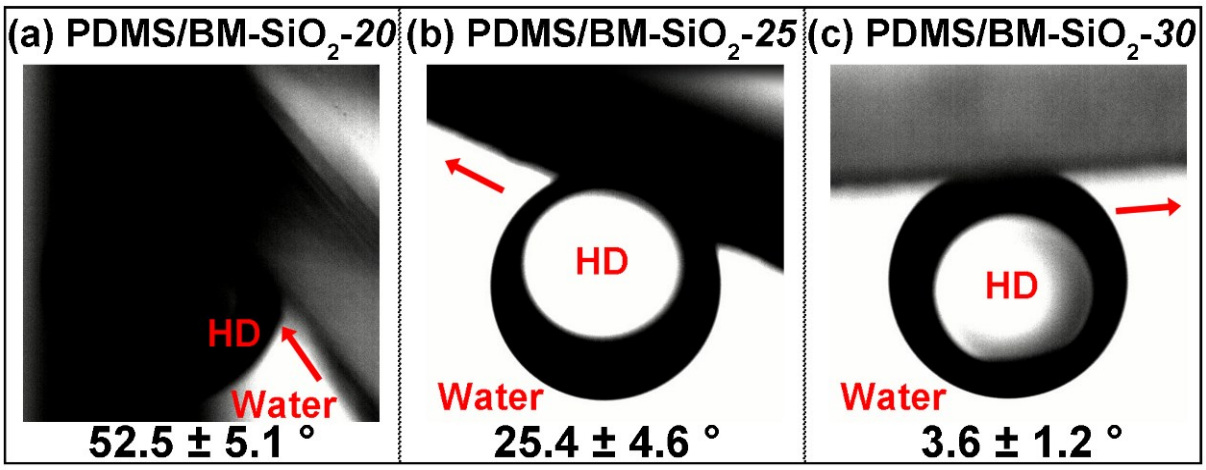

Fig. S9 Typical snapshot images of UWOSAs of (a) PDMS/BM-SiO_2-*20*, (b) PDMS/BM-SiO_2-*25* and (c) PDMS/BM-SiO_2-*30* (mean ± SD, n = 5).

Figure S10

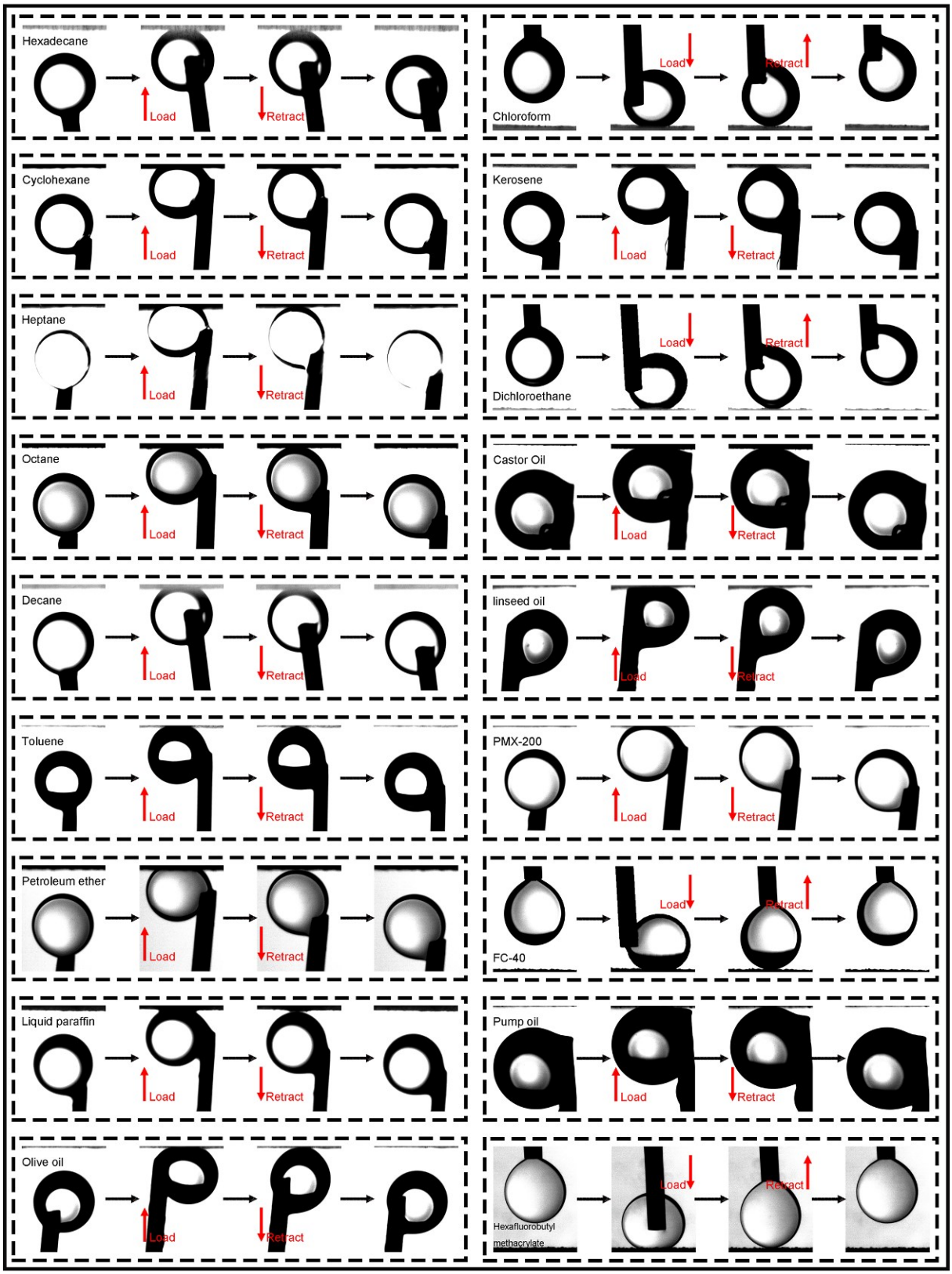

Fig. S10 Digital images recording the dynamic underwater oil-repellency on the surface of PDMS/BM-SiO_2-*30*.

Figure S11

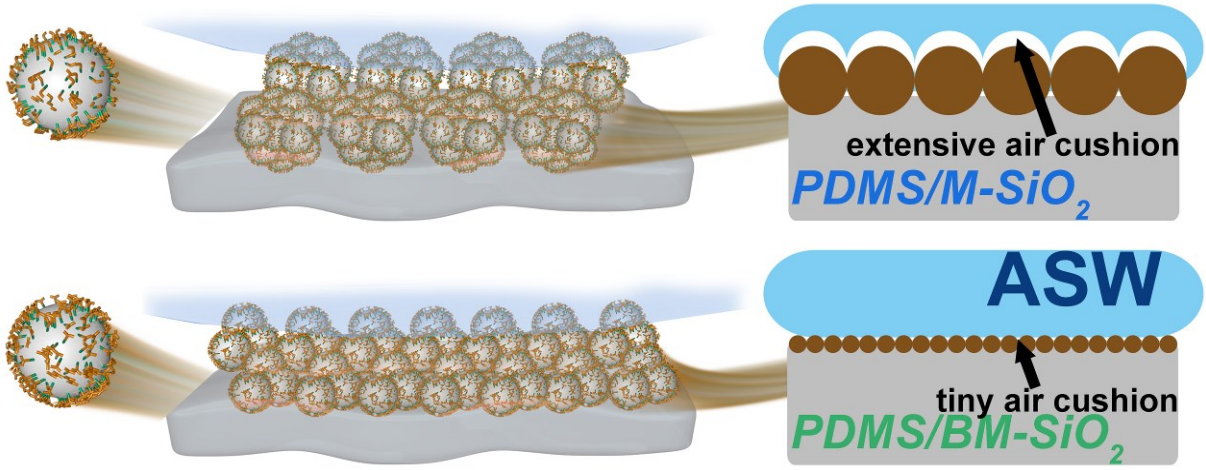

Fig. S11 Schematic illustrating the distinction of surface roughness between PDMS/M-SiO_2-*n* and PDMS/BM-SiO_2-*n*.

Figure S12

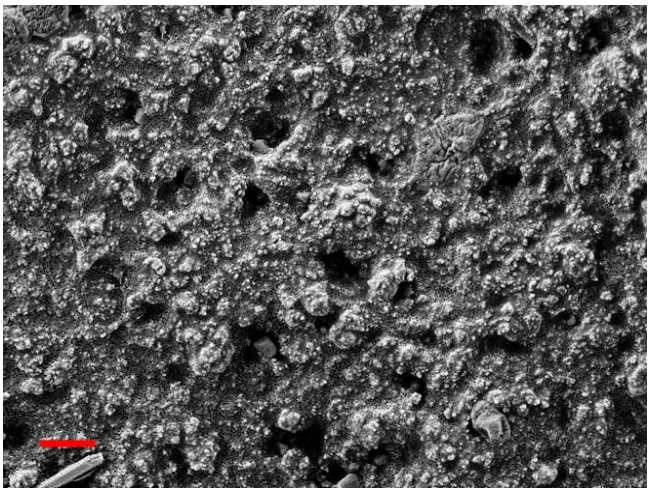

Fig. S12 FE-SEM image of PDMS/BM-SiO_2-*30* after immersed in ASW for 3 d and realized wettability switch from superhydrophobicity to underwater superoleophobicity. Scale bar: 1 μm.

Figure S13

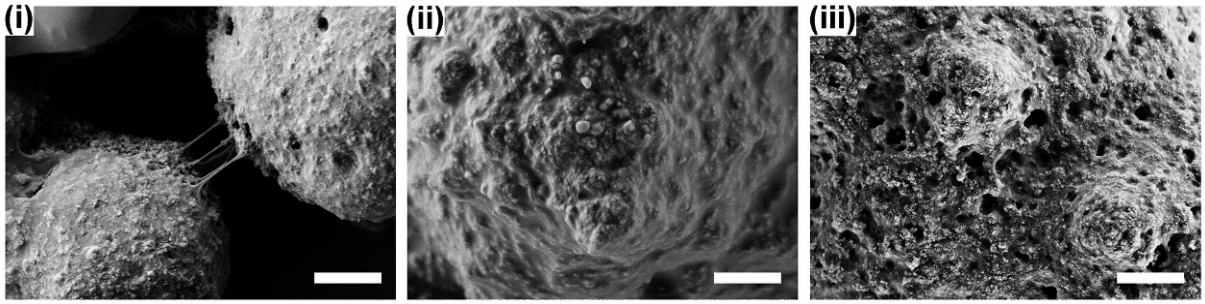

Fig. S13 FE-SEM images with high magnification of i) PDMS/SiO_2-*30*, ii) PDMS/M-SiO_2-*30* and iii) PDMS/BM-SiO_2-*30* after immersed in ASW for 5 months. Scale bar: 2 μm.

Figure S14

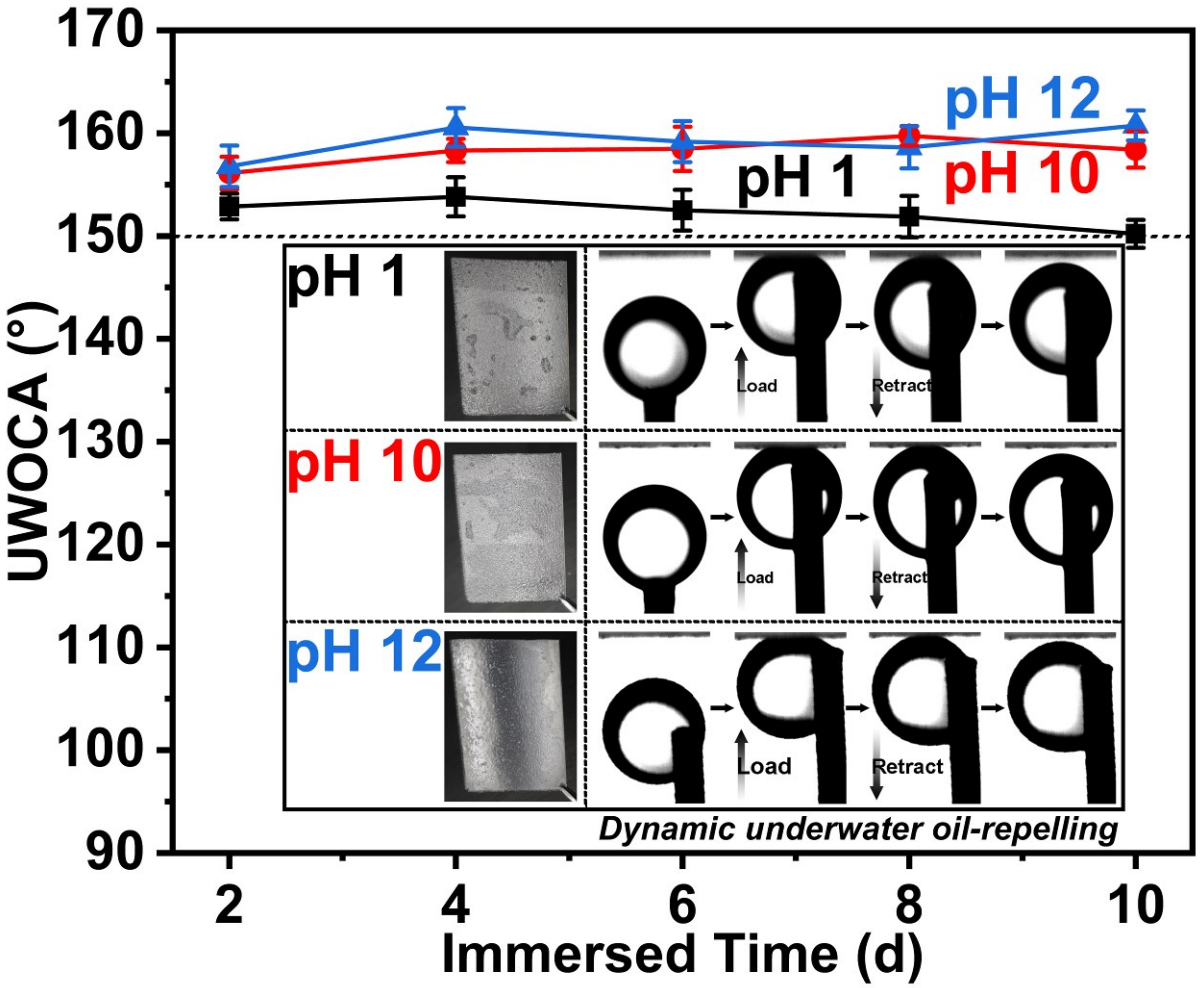

Fig. S14 Evolution of UWOCA of PDMS/BM-SiO_2-*30* during the immersion in solutions with different pH values. Inset solid frame shows the digital images and dynamic underwater oil-repellency after immersion for 10 d (mean ± SD, n = 5).

Figure S15

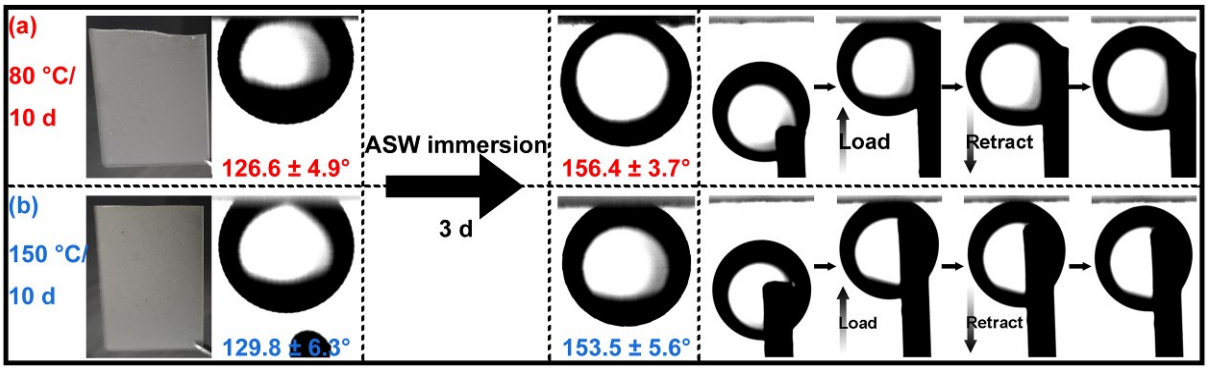

Fig. S15 Digital images and UWOCAs of PDMS/BM-SiO_2-*30* after stored at (a) 80 °C and (b) 150 °C for 10 d, and the corresponding UWOCAs and dynamic underwater oil-repellency after further immersed in ASW for 3 d (mean ± SD, n = 5).

Figure S16

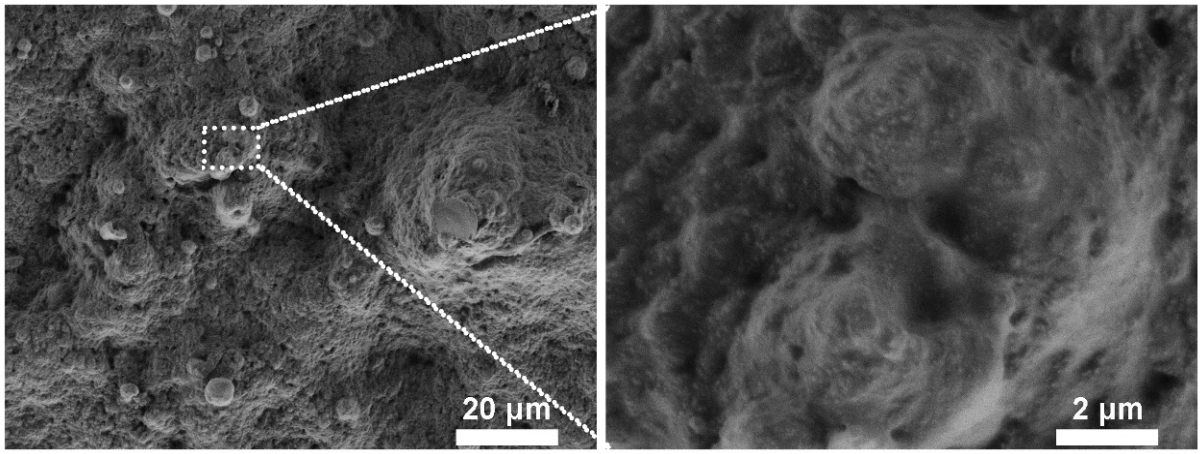

Fig. S16 FE-SEM images of PDMS/BM-SiO_2-*30* after 10 times of sandpaper abrasion (before immersing in ASW). The coating lost its initial underwater superoleophobicity, while the freshly exposed surface still remained in analogous micro/nanoscale texture as its original counterpart.

Figure S17

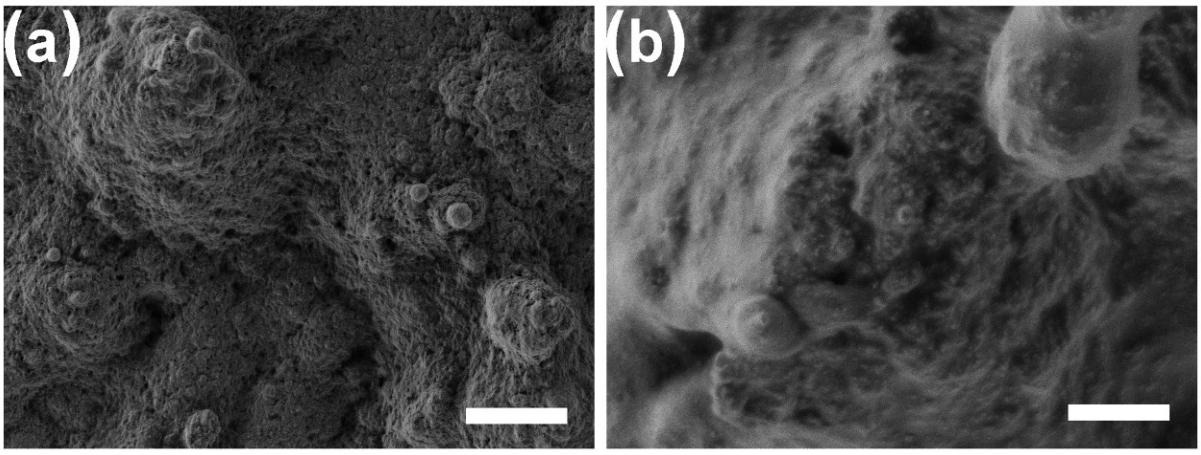

Fig. S17 FE-SEM images with (a) low (scale bar: 20 μm) and (b) high magnifications (scale bar: 2 μm) for PDMS/BM-SiO_2-*30* after the 10th cycle of mechanical abrasion-ASW immersion test. The surface maintained micro/nanoscale texture.

Figure S18

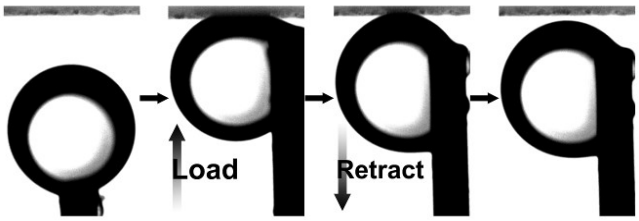

Fig. S18 Dynamic underwater oil-repellency on the surface of PDMS/BM-SiO_2-*30* after the 10th cycle of mechanical abrasion-ASW immersion test.

Figure S19

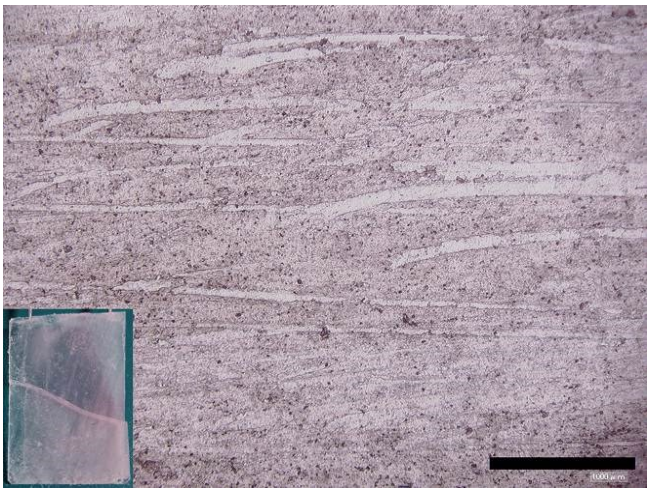

Fig. S19 Digital and OM images of PDMS/BM-SiO_2-*30* after the 13th cycle of mechanical abrasion-ASW immersion test. Scale bar: 1000 μm.

Figure S20

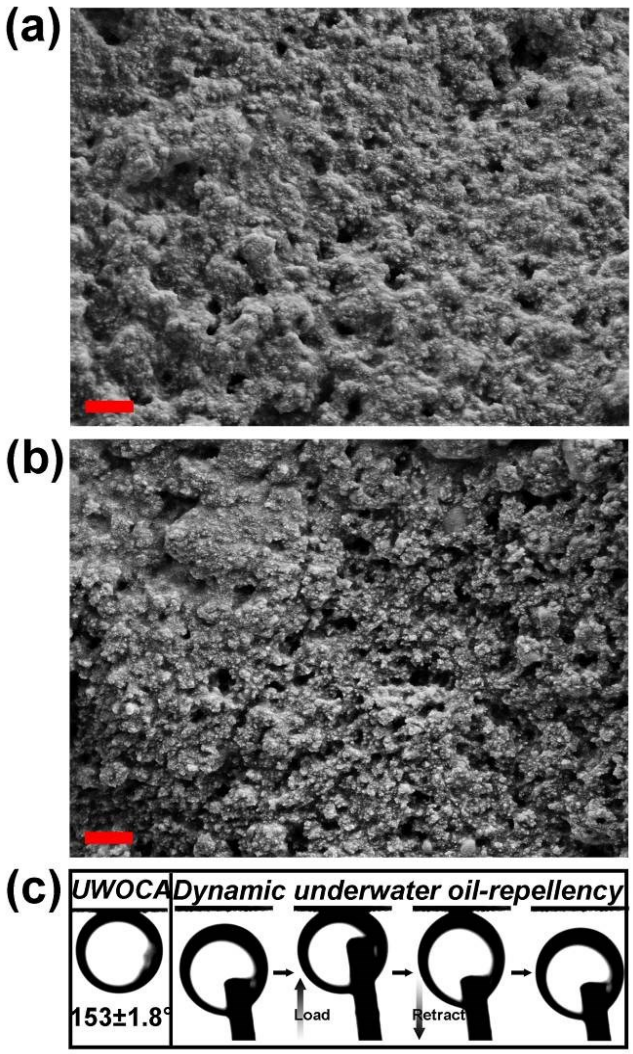

Fig. S20 Sandpaper abrasion test performed in air. FE-SEM images of PDMS/BM-SiO_2-*30* (a) after rubbed for 100 times and (b) later immersed in ASW for 3 d (c) to self-regenerate underwater superoleophobicity (mean ± SD, n = 5). Scale bar: 1 μm.

Figure S21

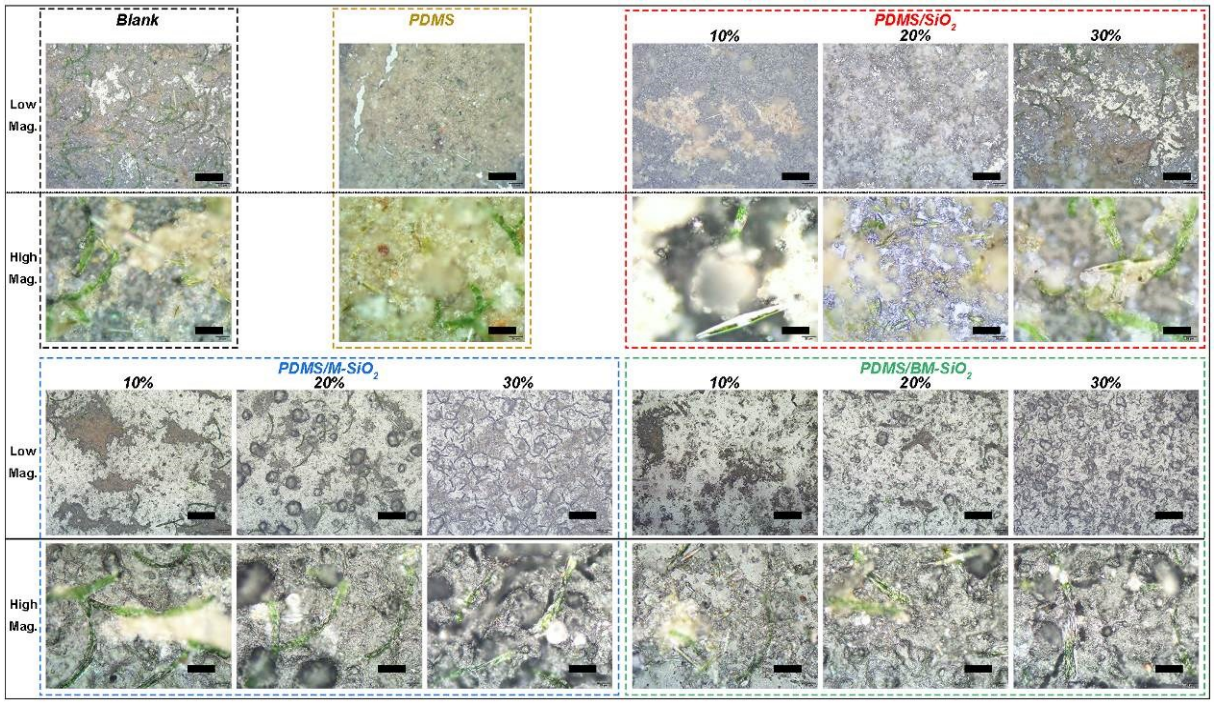

Fig. S21 OM images with high contrast to show the morphology of bio-contaminants after 14 d field exposure for blank glass, PDMS, PDMS/SiO_2-*n*, PDMS/M-SiO_2-*n* and PDMS/BM-SiO_2-*n* (scale bar: 200 μm and 40 μm for low and high mag., respectively).

Figure S22

Fig. S22 Details of marine field trials. a) Mold; b) experimental scene; c) immersing the samples.

References

1 X. Liang, X.-K. Zhang, L.-H. Peng, Y.-T. Zhu, A. Yoshida, K. Osatomi and J.-L. Yang, *Int. J. Mol. Sci.*, 2020, **21**, 710.

2 X. Liang, L.-H. Peng, S. Zhang, S. Zhou, A. Yoshida, K. Osatomi, N. Bellou, X.-P. Guo, S. Dobretsov and J.-L. Yang, *Chemosphere*, 2019, **218**, 599.